

# Reversible thermally-responsive electrochemical energy storage based on smart LDH@P(NIPAM-co-SPMA) films†

Cite this: *Chem. Commun.*, 2013, **49**, 8462

Received 24th April 2013,  
Accepted 23rd July 2013

DOI: 10.1039/c3cc43039a

[www.rsc.org/chemcomm](http://www.rsc.org/chemcomm)

Yibo Dou, Ting Pan, Awu Zhou, Simin Xu, Xiaoxi Liu, Jingbin Han, Min Wei,\*  
David G. Evans and Xue Duan

**A smart supercapacitor was fabricated by loading a thermosensitive polymer P(NIPAM-co-SPMA) onto the surface of NiAl-layered double hydroxide (LDH) nanowalls grown on a flexible Ni foil substrate, which displays temperature-triggered on-off ion channels for controlling the electrochemical behavior.**

With the ever-increasing power and energy needed for applications ranging from modern consumer electronics to micro systems and next-generation plug-in hybrid electric vehicles, advanced energy storage devices (*e.g.*, lithium ion batteries and supercapacitors) have been used to meet the tremendous power demands of energy storage systems.<sup>1,2</sup> Although considerable efforts have been devoted to investigate energy storage devices with advantages of fast charging–discharging, high power delivery and excellent cycling lifespan,<sup>3,4</sup> the self-safety of devices still remains a challenging goal and should be given special consideration. Since high power delivery and fast current flow are prone to generate a severe thermal effect that the working device cannot dissipate quickly, especially at high environmental temperature, thermal runaway may occur in such strongly exothermic systems.<sup>5</sup> This issue is regarded as a serious problem in the safety and controllability of power delivery. Therefore, the exploration of new materials or approaches to obtain novel energy storage devices with excellent charge storage properties and enhanced safety concomitantly for satisfying practical performance demands is an urgent problem that needs to be solved.

Smart materials based on stimuli-responsive polymers, capable of conformational and chemical changes induced by external signals, can be tailored to achieve expected performance requirements.<sup>6</sup> Recently, potential applications of smart materials in switchable sensors, electrochemical logic gates and signal storage/processing have attracted much interest,<sup>7,8</sup> but these have rarely been employed in electrical energy storage systems. Provided that the processes of electrochemical power delivery at a high

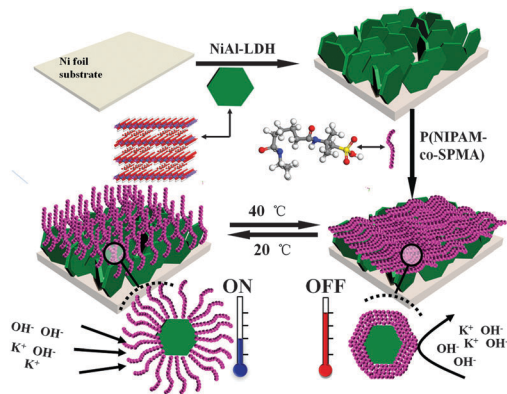
temperature can be commanded by a thermally-responsive material, the use of a smart electrical device would be a solution to the aforementioned safety and controllability issues in the energy storage field. As a result, it is essential to take up the challenge of developing smart energy storage devices with high stimuli-sensitivity and facile reversibility for guaranteeing the device safety.

Layered double hydroxides (LDHs) are a type of layered clay, which can be described by the general formula  $[M^{II}_{1-x}M^{III}_x(OH)_2](A^{n-})_{x/m} \cdot mH_2O$  ( $M^{II}$  and  $M^{III}$  are divalent and trivalent metals, respectively;  $A^{n-}$  is an interlayered anion).<sup>9,10</sup> Owing to the versatility in chemical composition and structural architecture, transition metal-based LDHs give rise to intriguing electrochemical properties which have attracted broad interests for application in biosensors, alkaline secondary batteries and supercapacitors.<sup>11,12</sup> Based on the above considerations, the combination of promising pseudocapacitive LDH materials and thermosensitive polymers would be a preferable solution to the fabrication of smart energy storage systems. Firstly, the electrochemically-active LDHs provide a well-organized and stable microenvironment for charge transfer to give high power density. Secondly, a thermosensitive polymer serves as an ion channel on the surface of LDHs, facilitates/inhibits the electrolyte transportation in the on-off state on account of its configuration change. This is expected to achieve the capacitance controllability and guarantee thermal safety simultaneously.

Herein, we demonstrate the fabrication of a novel LDH@P(NIPAM-co-SPMA) electrode by loading a thermosensitive polymer P(*N*-isopropylacrylamide-co-2-acrylamido-2-methyl propane sulfonic acid) (P(NIPAM-co-SPMA)) onto the surface of NiAl-layered double hydroxide (LDH) nanowalls grown on a flexible Ni foil substrate. The resulting supercapacitor shows temperature-triggered on-off ion channels for controlling the electrochemical performances (Scheme 1). Owing to the configuration variation of P(NIPAM-co-SPMA) upon changing the temperature, the collapsed polymer at 40 °C inhibits ion transport and thus weakens the power delivery, while the dissolved polymer at 20 °C releases the accessible ion channels for the normal charge–discharge process. Therefore, this work provides a promising strategy for the design and fabrication of thermally-responsive supercapacitors.

State Key Laboratory of Chemical Resource Engineering,  
Beijing University of Chemical Technology, Beijing 100029, P. R. China.  
E-mail: weimin@mail.buct.edu.cn; Tel: +86-10-64412131

† Electronic supplementary information (ESI) available: XRD; AFM; contact angles; UV-vis spectra; electrochemical tests including CVs and GV discharge curves. See DOI: 10.1039/c3cc43039a



**Scheme 1** Schematic illustration of the LDH@P(NIPAM-co-SPMA) film on a flexible Ni foil substrate serving as a smart supercapacitor with thermally-responsive ion channels.

Fig. S1 (ESI<sup>†</sup>) illustrates the XRD patterns of the LDH film on Ni foil and the corresponding powdered sample scraped from the substrate for comparison. The powdered material shows a series of reflections at  $2\theta$  11.8°, 23.5°, 35.4°, 39.2° and 46.8°, corresponding to the [003], [006], [012], [015] and [018] reflections of a randomly-stacked  $\text{CO}_3^{2-}$ -LDH phase, respectively.<sup>13</sup> For the arrayed LDH film, the absence of [00 $l$ ] reflections indicates a preferential orientation of LDH crystallites with their  $ab$  plane perpendicular to the substrate. The LDH film with uniform hexagonal plate-like microcrystals is shown in Fig. 1A, which shows an open-up network structure composed of interconnected nanoplatelet building blocks. A representative cross-sectional SEM image (Fig. 1A, inset) shows that the LDH film with an average lateral size of  $\sim 5.1 \mu\text{m}$  is approximately vertically aligned on the supporting substrate, which is consistent with the XRD results. The typical TEM image (Fig. 1B) displays the LDH with sheet-like morphology and micrometre size, with a lattice spacing of 0.26 nm (Fig. 1C) ascribed to the [012] crystal plane of the LDH material. The corresponding selected-area electron diffraction (SAED) pattern (Fig. 1C, inset) exhibits hexagonally-arranged bright spots, indicating its single-crystal nature. Upon coating the surface of the LDH film with a thin layer

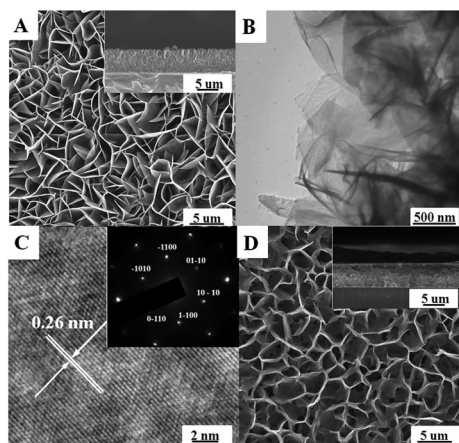


**Fig. 1** (A) Top-view and cross-sectional SEM image (inset) of NiAl-LDH arrayed film; (B) TEM image of NiAl-LDH nanowalls; (C) high-resolution TEM image of an individual LDH nanoplatelet and the corresponding SAED pattern (inset); (D) top-view and cross-sectional SEM image (inset) of the LDH@P(NIPAM-co-SPMA) film.

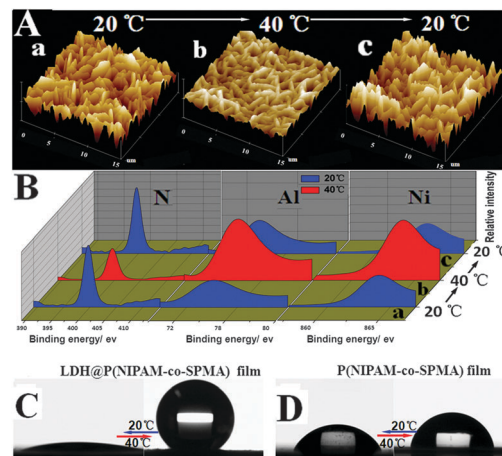


**Fig. 2** (A) AFM images and (B) XPS spectra (N 1s, Al 2p and Ni 2p peak, respectively) of the LDH@P(NIPAM-co-SPMA) film at various temperatures: from (a) 20 °C to (b) 40 °C and (c) back to 20 °C. Photographs of the water droplet on the surface of the (C) LDH@P(NIPAM-co-SPMA) film and the (D) P(NIPAM-co-SPMA) planar film at 20 °C and 40 °C, respectively.

of P(NIPAM-co-SPMA) polymer, no obvious change in surface morphology and film thickness was observed (Fig. 1D) for the resulting LDH@P(NIPAM-co-SPMA) film.

The temperature-triggered variation in surface topography for the LDH@P(NIPAM-co-SPMA) film was investigated by AFM. The root-mean-square roughness of the surface topography decreases from  $\sim 116.5 \text{ nm}$  to  $\sim 38.5 \text{ nm}$  during the heating process from 20 °C to 40 °C, and then increases to  $\sim 120.3 \text{ nm}$  after cooling to 20 °C (Fig. 2A). X-ray-photoelectron spectroscopy (XPS) was further employed to analyze the surface composition in response to temperature. As shown in Fig. 2B, the relative ratio of N/(Al + Ni) is 32.1%/67.9% at 20 °C, but it decreases to 10.3%/89.7% after heating to 40 °C and then recovers to 34.4%/65.6% as the temperature drops to 20 °C. This reversible process is related to the configurational change of P(NIPAM-co-SPMA). This thermosensitive polymer domain exhibits an expanded state at 20 °C, accounting for the less smooth surface and increased relative ratio of N/(Al + Ni); in contrast, a more smooth surface and decreased N/(Al + Ni) ratio were obtained at 40 °C owing to the collapse of the P(NIPAM-co-SPMA) domain. In addition, a transition of the water contact angle (CA) for the LDH@P(NIPAM-co-SPMA) film from  $\sim 16^\circ$  to  $\sim 140^\circ$  is observed as the temperature rises from 20 °C to 40 °C (Fig. 2C). In contrast, a pristine P(NIPAM-co-SPMA) film only shows a relatively narrow CA change ( $57\text{--}78^\circ$ ) (Fig. 2D), which is consistent with the previously reported value.<sup>8</sup> This significant enlargement of the CA response range is attributed to the geometric amplification effect on wetting properties imposed by the highly arrayed LDH wall.<sup>8</sup> The difference in the value of CA in response to temperature (Fig. S2, ESI<sup>†</sup>) further indicates a significant variation in the thermal-stimuli surface wetting for the LDH@P(NIPAM-co-SPMA) film. The sharp change in CA at  $\sim 30 \text{ }^\circ\text{C}$  is attributed to the thermal phase transition behavior of P(NIPAM-co-SPMA) (Fig. S3, ESI<sup>†</sup>), with a high reversibility as confirmed by five consecutive heating-cooling cycles between 20 °C and 40 °C (Fig. S4, ESI<sup>†</sup>). The reversible variation in surface topography, composition and wettability induced by temperature stimuli would in turn affect the electrochemical performance of the film as an electrode, which will be discussed in the next section.

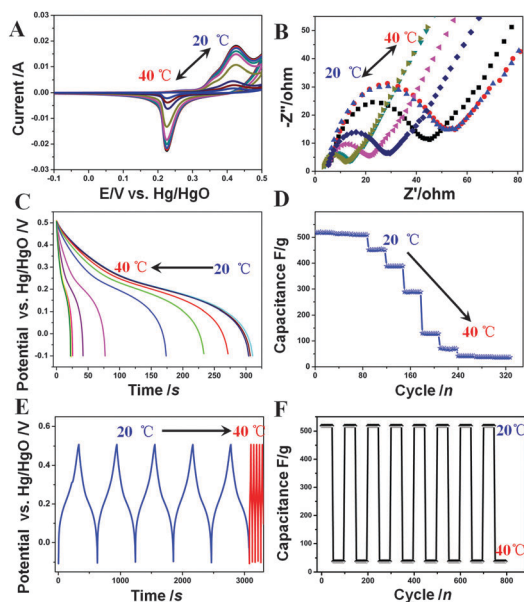


**Fig. 3** Temperature-dependent (A) CVs, (B) EIS, (C) GV discharge curves and (D) specific capacitance in the range 20–40 °C of the LDH@P(NIPAM-co-SPMA) electrode; (E) the GV charge–discharge curves with the increase of temperature from 20 °C to 40 °C; (F) the specific capacitance of the thermally-responsive LDH@P(NIPAM-co-SPMA) switch between 20 °C and 40 °C for eight heating–cooling cycles.

The electrochemical tests as a function of temperature were performed to investigate the thermally-responsive capacitive performance of the LDH@P(NIPAM-co-SPMA) electrode.

As the temperature increases from 20 °C to 40 °C, a progressive decrease in both the anodic and cathodic peak currents is observed in the cyclic voltammogram (CV) curves (Fig. 3A), and the plot of specific capacitance vs. temperature (Fig. S5, ESI<sup>†</sup>) demonstrates two stable states at 20 °C and 40 °C, respectively. However, no obvious CV change for both the LDH film and the LDH@P(SPMA) film was observed upon increasing the temperature from 20 °C to 40 °C (Fig. S6, ESI<sup>†</sup>), indicating that pNIPAM plays a key role in determining the thermally-responsive behavior of the supercapacitor. In addition, the results obtained using impedance spectroscopy (EIS) in the temperature range 20–40 °C (Fig. 3B) further provide more information about the interfacial impedance change. The diameter of the semicircle in the EIS response becomes larger upon increasing the temperature, indicating a decreased interfacial charge transfer of the electrode at high temperature due to the contraction state of the P(NIPAM-co-SPMA) polymer.

Subsequently, the constant-current galvanostatic (GV) charge–discharge curves of the LDH@P(NIPAM-co-SPMA) electrode at varied temperatures were measured. The electrode exhibits a constant decrease in the specific capacitance from  $\sim 518 \text{ F g}^{-1}$  to  $\sim 38 \text{ F g}^{-1}$  as the temperature rises from 20 °C to 40 °C (Fig. 3C and D), while the specific capacitance of the randomly-stacked LDH/P(NIPAM-co-SPMA) electrode as a comparison sample merely decreased from  $\sim 505 \text{ F g}^{-1}$  to  $\sim 361 \text{ F g}^{-1}$  (Fig. S7, ESI<sup>†</sup>), demonstrating that the highly-arrayed LDH nanowalls are essential to the polymer phase transition and

the largely-enhanced sensitivity. The GV charge–discharge curves for the LDH@P(NIPAM-co-SPMA) switch at 20 °C and 40 °C (Fig. 3E) display a largely-depressed electrochemical capacitive performance at 40 °C, owing to the closure of ion channels. Moreover, the specific capacitance of the switch at 20 °C and 40 °C manifests a highly-reversible transition (Fig. 3F). The bending LDH@P(NIPAM-co-SPMA) electrode exhibits almost the same specific capacitance as the unbent sample, as well as excellent thermal controllability (Fig. S8, ESI<sup>†</sup>), indicating its capability as a flexible energy storage device. In addition, in the test for long-term stability, the LDH@P(NIPAM-co-SPMA) electrode maintains  $\sim 98\%$  of its initial specific capacitance value after 50 days (Fig. S9, ESI<sup>†</sup>), which should guarantee its practical applications.

In summary, a facile and cost-effective approach has been developed to fabricate a thermally-responsive supercapacitor based on a highly-arrayed LDH@P(NIPAM-co-SPMA) film. The film exhibits reversible variation in surface topography, composition and wettability induced by temperature-controlled configuration change of the P(NIPAM-co-SPMA) polymer. The electrochemical capacitive performance of smart supercapacitors can be switched by reversible on–off ion channels at 20 °C and 40 °C, which is expected to achieve thermal safety and capacitance control in an electrical energy storage device. Therefore, the strategy in this work provides a promising approach to address the thermal runaway problem in energy storage devices, which display potential applications in switchable sensors, actuators and supercapacitors.

This work was supported by the National Natural Science Foundation of China (NSFC), the 973 Program (Grant No. 2011CBA00504) and the Fundamental Research Funds for the Central Universities (Grant No.: ZY1215). M. Wei particularly appreciates the financial aid from the China National Funds for Distinguished Young Scientists of the NSFC.

## Notes and references

- L. Dai, D. W. Chang, J. B. Baek and W. Lu, *Small*, 2012, **8**, 1130.
- P. Simon and Y. Gogotsi, *Nat. Mater.*, 2008, **7**, 845.
- Y. He, G. Li, Z. Wang, C. Su and Y. Tong, *Energy Environ. Sci.*, 2011, **4**, 1288.
- X. Lang, A. Hirata, T. Fujita and M. Chen, *Nat. Nanotechnol.*, 2011, **6**, 232.
- L. Xia, S. Li, X. Ai, H. Yang and Y. Cao, *Energy Environ. Sci.*, 2011, **4**, 2845.
- H. Wu, J. Dong, C. Li, Y. Liu, N. Feng, L. Xu, X. Zhan, H. Yang and G. Wang, *Chem. Commun.*, 2013, **49**, 3516.
- P. Wan, Y. Xing, Y. Chen, L. Chi and X. Zhang, *Chem. Commun.*, 2011, **47**, 5994.
- (a) H. Ko, Z. Zhang, Y. Chueh, E. Saiz and A. Javey, *Angew. Chem., Int. Ed.*, 2010, **49**, 616; (b) D. Phillips and M. Gibson, *Chem. Commun.*, 2012, **48**, 1054.
- (a) M. Shao, M. Wei, D. G. Evans and X. Duan, *Chem. Commun.*, 2011, **47**, 3171; (b) S. Gago, T. Costa, J. S. de Melo, I. S. Gonçalves and M. Pillinger, *J. Mater. Chem.*, 2008, **18**, 894.
- F. Leroux and C. Taviot-Gu  ho, *J. Mater. Chem.*, 2005, **15**, 3628.
- A. I. Khan, L. X. Lei, A. J. Norquist and D. O'Hare, *Chem. Commun.*, 2001, 2342.
- J. Han, Y. Dou, J. Zhao, M. Wei, D. G. Evans and X. Duan, *Small*, 2013, **9**, 98.
- J. Han, J. Lu, M. Wei, Z. L. Wang and X. Duan, *Chem. Commun.*, 2008, 5188.